jmr&t
Journal of Materials Research and Technology
www.jmrt.com.br

Original Article

Photoluminescence and semiconducting behavior of Fe, Co, Ni and Cu implanted in heavy metal oxide glasses

Mohamed A. Marzouk[a,*], Sherief M. Abo-Naf[a], Hamdia A. Zayed[b], Nevien S. Hassan[c]

[a] Glass Research Department, National Research Centre, Giza, Egypt
[b] Physics Department, Faculty of Girls, Ain-Shams University, Cairo, Egypt
[c] Egyptian Organization for Standardization and Quality (EOS), Cairo, Egypt

ARTICLE INFO

Article history:
Received 9 April 2015
Accepted 1 November 2015
Available online 17 December 2015

Keywords:
Glass
Heavy metal
Transition metal
Photoluminescence
Band gap
Urbach energy

ABSTRACT

Transition metal ions (0.5 wt%) of Fe_2O_3, CoO, NiO or CuO doped heavy metal oxide glasses having chemical composition of $60PbO{\cdot}20Bi_2O_3{\cdot}20\,M_xO_y$ mol% (where $M_xO_y = B_2O_3$ or SiO_2 or P_2O_5) were prepared by conventional melt annealing method. Combined optical and photoluminescence properties have been measured and employed to evaluate the prepared glassy samples. From the absorption edge data, the values of the optical band gap E_{opt}, Urbach energy (ΔE) and refractive index were calculated to estimate semiconducting behavior. Photoluminescence and values of the optical energy gap were found to be dependent on the glass composition. The variations of the photoluminescence intensity, values of optical band gap, Urbach energy and refractive index gave an indication to use the prepared glasses for design of novel functional optical materials with higher optical performance.

1. Introduction

Transition metals doped glasses have found an interest in many areas of application. Such glasses are good materials for use in optical, electric, thermal, and mechanical applications. Transition metal ions are characterized by partially filled d-shell that can frequently exist in a number of oxidation states and the electro-optical behavior can occur as a result of electron transfers from ions in a lower to those in a higher oxidation state [1]. Many studies [1–3] have pointed out the relationships between the structure of the host glass and the properties of the doped ions that, in turn, help for designing of glasses for different applications. The current interest in transition metal or rare earth ions doped glasses is mainly for two reasons: firstly, their well defined and sharp energy levels may serve as structural probes for the environment of the dopant, and secondly, the modifications of the energy level structure of the rare earth ions caused by the glassy environment may lead to interesting applications [1,3]. Recently, heavy metal oxides such as Bi_2O_3 and PbO have been added to the conventional glass systems in order to enhance the opti-

* Corresponding author.
E-mail: marzouk_nrc@yahoo.com (M.A. Marzouk).
http://dx.doi.org/10.1016/j.jmrt.2015.11.003

cal and mechanical behavior. Bismuth-doped glasses show various emission centers at wavelengths ranging from 400 to 2500 nm [4,5]. Therefore, these glasses are very promising optical materials for photonic as well as optoelectronic applications. The transition metals doped bismuth glasses show enhanced photoluminescence. These enhanced photoluminescence were observed due to energy transfer mechanism from the above ionic species to bismuth. In addition, bismuth containing glasses are used in the electronic field due to the low field strength and high polarizability of Bi^{3+} ions [6]. This property makes these glasses very useful in optical memory devices.

In the present work, iron, cobalt, nickel and copper ions, implanted in host lead and bismuth heavy metal oxide glasses, were doped with low amounts of common glass formers, i.e. borate, silicate and phosphate. UV–visible absorption and photoluminescence were determined for the prepared glasses. It is also very important to investigate optical band gap and the refractive index to detect the semiconducting behavior of such glasses.

2. Experimental details

2.1. Preparation of glasses

The glasses were prepared from chemically pure materials. Orthoboric acid (H_3BO_3) was used for B_2O_3, SiO_2 was introduced as pulverized quartz, P_2O_5 was introduced in the form of $NH_4H_2PO_4$, Pb_3O_4 was used for PbO and Bi_2O_3 was introduced as such. Transition metals (Fe_2O_3, CoO, NiO or CuO) were added (0.5 wt%) in the form of their respective oxides to the base undoped lead bismuth borate, silicate and phosphate. The accurately weighed batches having chemical composition of $60PbO–20Bi_2O_3–20\,M_xO_y$ mol% (where $M_xO_y = B_2O_3$ or SiO_2 or P_2O_5) were melted in alumina crucibles at 1150–1200 °C for 1 h to achieve homogeneous and clear samples. The crucibles were rotated at intervals to promote chemical and physical homogeneity of the melts. After complete fining, the melts were cast into warmed stainless steel molds of required dimensions. The prepared glasses were immediately transferred to a muffle furnace regulated at 350 °C for annealing. After 1 h, the muffle furnace, with the glasses inside, was left to cool down to room temperature at a rate of 25 °C/h.

2.2. UV–visible absorption spectra

Optical (UV–visible) absorption spectral measurements were performed using an UV-VIS spectrophotometer (type T80, PG Instruments, England). The range of measurement was from 200 to 1100 nm. Perfectly polished samples of the dimensions 1 cm × 1 cm × 0.2 cm were measured twice to confirm the accuracy of the absorption peaks. The irradiated glasses were immediately measured after the irradiation process.

2.3. Photoluminescence spectra

Photoluminescence emission spectra were recorded at room temperature using a fluorescence spectrophotometer type (Jasco FP-6500, Japan) equipped with a xenon flash lamp as the excitation light source. The scan speed is 0.1 s $step^{-1}$ with a step length of 0.25 nm and a slit width of 0.2 nm.

2.4. Optical band gap energy (E_{opt}) and Urbach energy (ΔE)

There are two types of optical transitions: direct and indirect. They can occur at the fundamental absorption edge of crystalline and non-crystalline semiconductor.

In both cases, electromagnetic waves interact with the electrons in the valence band, which are raised across the fundamental gap to the conduction band [7]. In order to determine the optical band gap for such glasses, Mott and Davis [8] have suggested the following expression for the relation between the optical band gap, absorption coefficient and energy ($h\nu$) of the incident photon:

$$\alpha h\nu = B(h\nu - E_{\text{opt}})^n \tag{1}$$

where E_{opt} is the optical energy gap, B is a constant called the band tailing parameter and n is an index which can be assumed to have values of 1/2, 3/2, 2 and 3, depending on the nature of the electronic transition responsible for the absorption. $n = 1/2$ for allowed direct transition, $n = 3/2$ for forbidden direct transition and $n = 3$ for forbidden indirect transition, with $n = 2$ refers to indirect allowed transitions [9].

Using the above Eq. (1), by plotting $(\alpha h\nu)^{1/2}$ as a function of photon energy $h\nu$, one can find the optical energy band gaps (E_{opt}) for indirect transition.

The Urbach energy gives the width of the tails of the localized states within the optical band gap [10]. The dependence of the absorption coefficient in the region of lower photon energy of the absorption edge can be described by the following formula [11]:

$$\alpha(\nu) = B\,\exp\left(\frac{h\nu}{\Delta E}\right) \tag{2}$$

where B is the constant, ΔE is the Urbach energy and υ is the frequency of radiation. Plots were also drawn between $\ln(\alpha)$ and $h\nu$ (Eq. (2)) and from these plots, the value of the Urbach energy ΔE can be calculated from the reciprocal of the slope of the linear portion of such plots.

The refractive index, n, can be calculated from the value of E_g using the formula proposed by Dimitrov and Sakka [12] as follows:

$$\frac{n^2-1}{n^2+2} = 1 - \sqrt{\frac{E_g}{20}} \tag{3}$$

3. Results and discussion

3.1. UV–visible absorption spectra

Figs. 1–4 illustrate the UV–visible absorption spectra of Fe_2O_3, CoO, NiO or CuO doped lead bismuth borate, silicate and phosphate glasses, respectively. According to our previous study [13], the undoped glasses show three UV absorption bands at about 235, 305 and 390 nm and an intense near-visible at about 435 nm. The observed strong UV absorption spectral bands

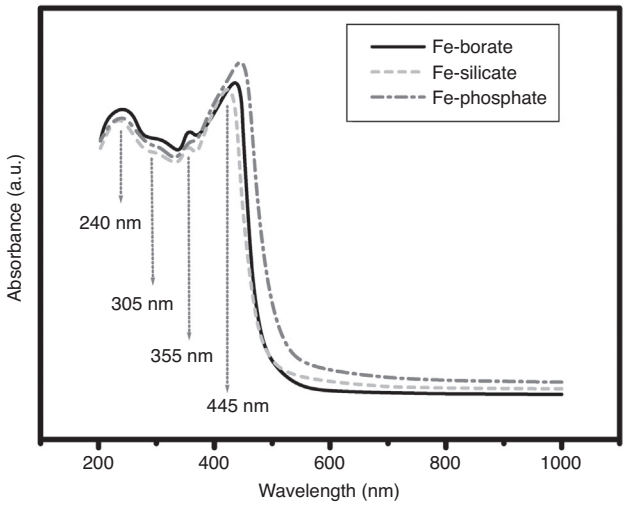

Fig. 1 – Absorption spectra of Fe-doped glasses.

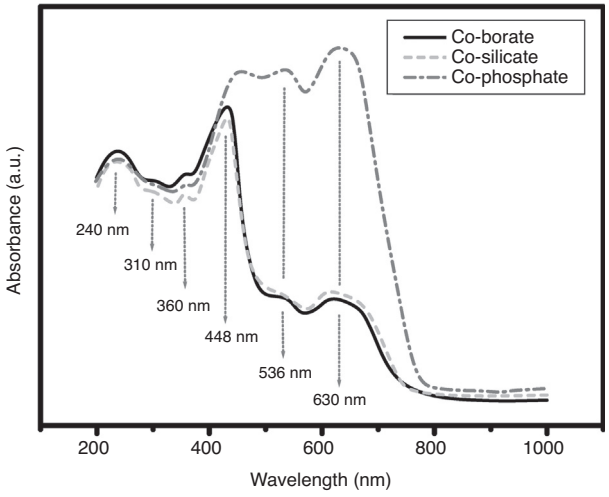

Fig. 2 – Absorption spectra of Co-doped glasses.

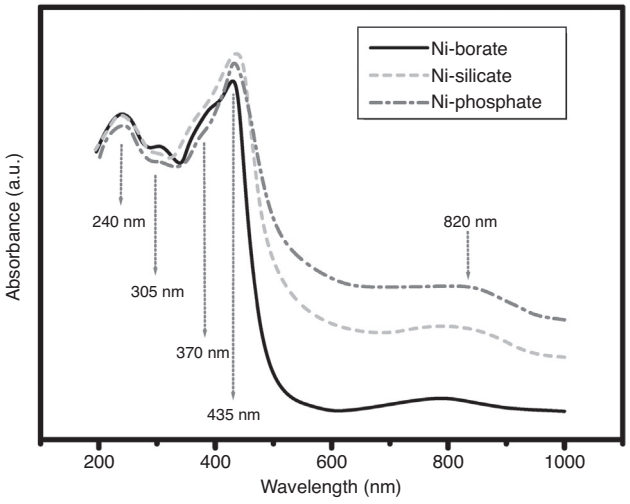

Fig. 3 – Absorption spectra of Ni-doped glasses.

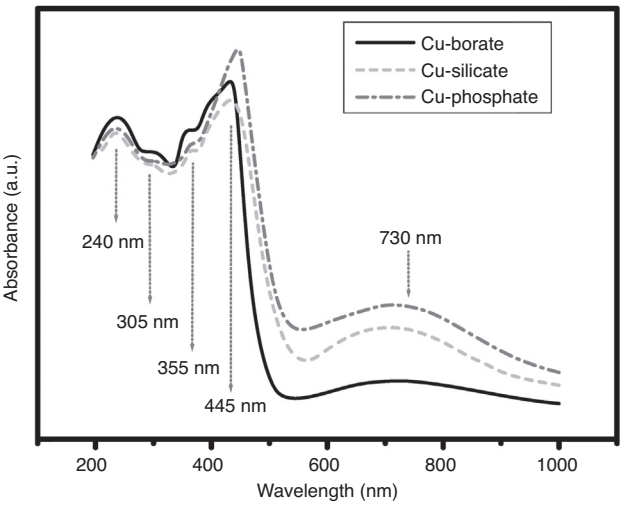

Fig. 4 – Absorption spectra of Cu-doped glasses.

from all studied glasses are primarily due to absorption of ferric (Fe^{3+}) ions present as trace impurities beside extra bands within the UV near visible region in the prepared glasses from the sharing absorption spectra of Pb^{2+} and Bi^{3+} ions in the UV-near visible region [14–18].

The optical spectrum of transition metal ions doped glasses can be summarized as follows.

3.1.1. *Fe_2O_3 doped glasses*

Fig. 1 illustrates the UV–visible absorption spectra of Fe_2O_3-doped glasses, which reveal three strong and broad UV absorption band centered at about 240, 305 and 355 nm, followed by a broad asymmetrical near-visible band centered at about 445 nm. The band at 445 nm is resolved due to the addition of 0.5% of Fe_2O_3 as dopant to the composition of the host glass, indicating its relationship to ferric ions (Fe^{3+}) added, and is assigned to the transitions $^6A_{1g}(S) \rightarrow {}^4A_{1g}(G) + {}^4E_g(G)$ [19].

3.1.2. *CoO doped glasses*

Fig. 2 represents the UV–visible absorption spectra of CoO-doped glasses, which reveal three strong and broad UV absorption band centered at about 240, 310 and 360 nm. This is followed by a very broad three visible absorption peaks at 448, 536 and 630 nm. The observed visible peaks are related to the presence of cobalt ions in the divalent state in two coordinations, the octahedral is identified at about 450 nm and the tetrahedral coordination at about 536 and 630 nm. The presence of two coordination states at the same time can be related to the similarity of the ligand stabilization energies of the two coordination states as reported by several authors [14,15,20].

3.1.3. *NiO doped glasses*

Fig. 3 shows the UV–visible absorption spectra of NiO-doped glasses, which reveal three strong and broad UV absorption band centered at about 240, 305 and 370 nm. The extended visible absorption band at about 820 nm can be attributed to the presence of Ni^{2+} ions ($3d^8$ configuration) of spin allowed transition $^3A_{2g}(^3F) \rightarrow {}^3T_{1g}(^3F)$ [21,22].

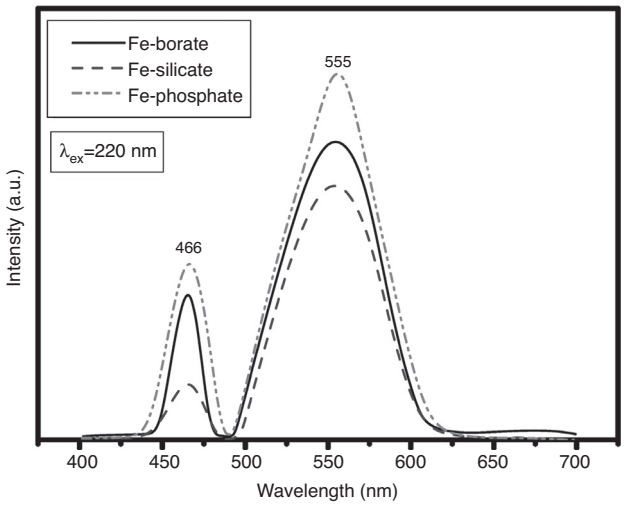

Fig. 5 – Emission spectra of Fe_2O_3-doped glasses.

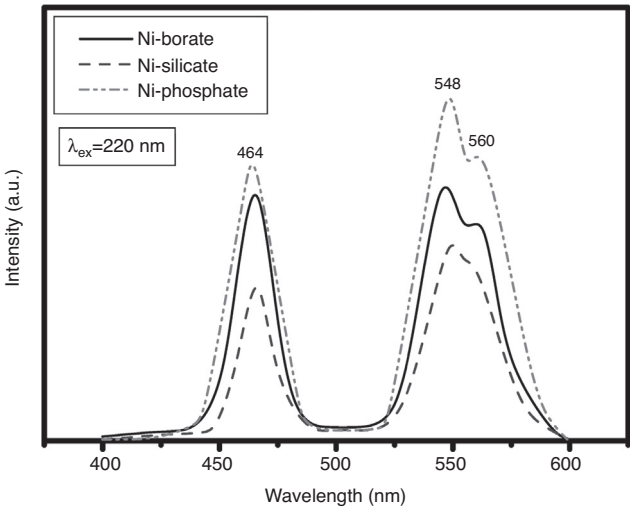

Fig. 7 – Emission spectra of NiO-doped glasses.

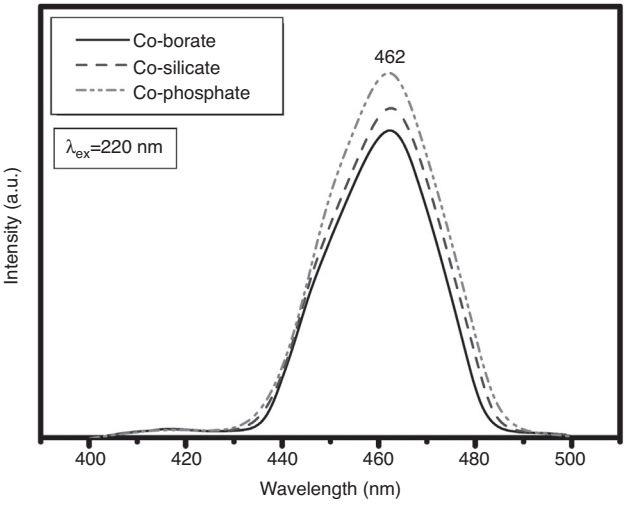

Fig. 6 – Emission spectra of CoO-doped glasses.

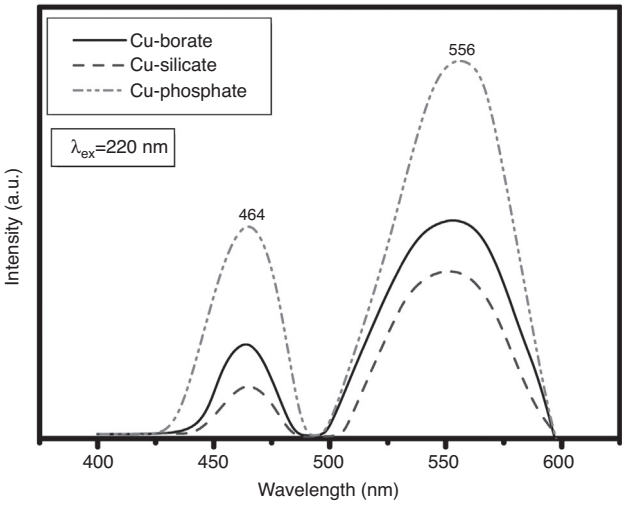

Fig. 8 – Emission spectra of CuO-doped glasses.

3.1.4. *CuO doped glasses*

Fig. 4 depicts the UV–visible absorption spectra of CuO-doped glasses, which reveal three strong and broad UV absorption band centered at about 240, 305 and 355 nm. The absorption broad band centered at 794 nm is related to the divalent copper ions (Cu^{2+}) in octahedral coordination and is assigned to the $^2B_{1g} \rightarrow {}^2B_{2g}$ transition of Cu^{2+} ions [14,15,20].

3.2. *Photoluminescence spectra*

Heavy metal bismuth ions doped conventional glass formers exhibit two characteristic emission peaks centered at about 465 and 550 nm which is usually attributed to $^1S_0 \rightarrow {}^3P_0$ or $^3P_2$ (spin forbidden) or $^1S_0 \rightarrow {}^3P_1$ or $^1P_1$ (spin–orbit coupling transitions) [13].

Figs. 5–8 show the emission spectra of heavy metal oxide glasses containing low concentrations of borate, silicate and phosphate glass formers, and doped with Fe_2O_3, CoO, NiO or CuO. The observed emission spectra, at 220 nm excitation, show two strong emission bands at about 462 and 550 nm for iron, nickel and copper doped glasses, while CoO doped glasses possess one emission band centered at about 462 nm. The intensity of the emission bands was found to be dependent on both of the type of glass former and the transition metal ion.

3.2.1. *Photoluminescence spectra of Fe_2O_3 doped glasses*

The emission spectra of 0.5% Fe_2O_3-doped samples, excited at 220 nm (in Fig. 5), show two strong broad emission bands extending nearly from 435 to 625 nm in the visible light range; the first emission peak is centered at 466 nm, and the other is centered at 555 nm.

It is accepted that iron can exist in glasses in two valences, namely Fe^{2+} and Fe^{3+}, and the ratios of them depend on the glass composition and conditions of melting [10,23]. It is well-known that the visible luminescence, related to deep level emissions, mainly results from defects such as interstitials and oxygen vacancies. According to Manjari et al. [24] the spectra of Fe(III) ions exhibit two emission bands which are: a strong UV emission band at 373 nm and a relatively weak blue

emission band at 450 nm, which are assigned to the transitions $^4T_{2g}(D) \rightarrow {}^6A_{1g}(S)$ and $^4A_{1g}(G) \rightarrow {}^6A_{1g}(S)$, respectively.

3.2.2. *Photoluminescence spectra of CoO doped glasses*

The emission spectra of 0.5% CoO-doped samples, excited at 220 nm (in Fig. 6), show only one strong broad emission band centered at about 462 nm.

It is fairly accepted that cobalt exists in glasses mostly in the divalent state with two coordinations, namely the octahedral and tetrahedral ones [10,23]. The Co^{2+} ion has a d^7 electronic configuration and in a tetrahedral crystal field presents the splitting of the energy levels of a d^3 electronic configuration in an octahedral field. In octahedral coordination (Co^{2+}) free ion ground state 4F splits into the $^4T_1$, $^4T_2$ and $^4A_2$ states with the $^4T_1$ state as the lowest one. In a tetrahedral symmetry, the energy levels of Co^{2+} ions are $^4T_2(4F)$, $^4T_1(4F)$, $^2E(2G)$ and $^4T_1(4P)$, etc., with the ground state of $^4A_2(4F)$. The emission band of Co^{2+} ions in the region 600–700 nm is assigned to $^2E(2G) \rightarrow {}^4A_2(4F)$ of Co^{2+} ions in tetrahedral coordination [21,25,26].

According to Naresh et al. [27] Co-doped glasses exhibited two emission bands of Co-doped glasses in the visible region which were attributed to $^4T_1(4P) \rightarrow {}^4A_2(4F)$ and $^4T_1(4P) \rightarrow {}^4T_2(4F)$ tetrahedral transitions of Co^{2+} ion.

Therefore, it is accepted that the origin of the emission bands of Co-doped glasses can be related not only to the presence of transition metal ion cobalt but also to the effect of heavy metal ions. Previous study [13] showed that the heavy metal ion Bi^{3+} is a very promising luminescent material and its emission peak is not located in one characteristic spectral region but varies from the ultraviolet region into the red region with differing host glass matrix. Bismuth doped borate, phosphate and silicate exhibit fluorescence emission centered at about 400 nm [13]. Consequently, the emission peak observed in the present results at 462 nm in case of CoO-doped glasses can be ascribed to Bi^{3+} ions matching with those attributions mentioned in Ref. [13].

3.2.3. *Photoluminescence spectra of NiO doped glasses*

The emission spectra of 0.5% NiO-doped glasses, excited at 220 nm (in Fig. 7), show three strong broad emission bands centered at about 464, 548 and 560 nm.

Ni^{2+} ions ($3d^8$) are expected to exist as octahedral and tetrahedral coordination sites within the glass matrix [10,23]. Furthermore, the energy levels of the excitation states of Ni^{2+} are different with the matrices change. The luminescence of Ni^{2+} ions doped glasses could be associated with the d–d optical transitions. It was reported [21,25,28] that energy levels of Ni^{2+} ions in octahedral symmetry are $^3A_{2g}(F) \rightarrow {}^4T_{2g}(F)$, $^3A_{2g}(F) \rightarrow {}^3T_{1g}(F)$ and $^3A_{2g}(F) \rightarrow {}^3T_{1g}(P)$. In addition to these three spin allowed transitions, a spin forbidden transition $^3A_{2g}(F) \rightarrow {}^1E_g(D)$ can be observed.

Many authors [21,25,28] have proposed that the luminescence properties of Ni-doped glasses exist in two regions, which are the green (577 nm) and red (670 nm) regions. Hence, according to the energy levels of Ni^{2+} ions transitions in octahedral sites, the emissions in green and red regions are assigned to the $^1T_{2g}(D) \rightarrow {}^3A_{2g}(F)$ and $^1T_{2g}(D) \rightarrow {}^3T_{2g}(F)$ transitions.

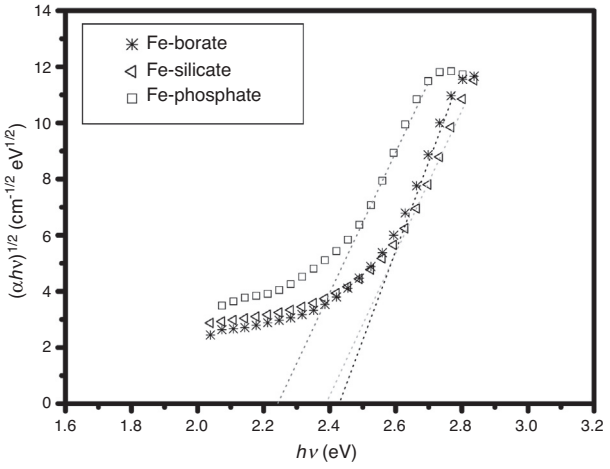

Fig. 9 – Optical band gap of Fe_2O_3-doped glasses.

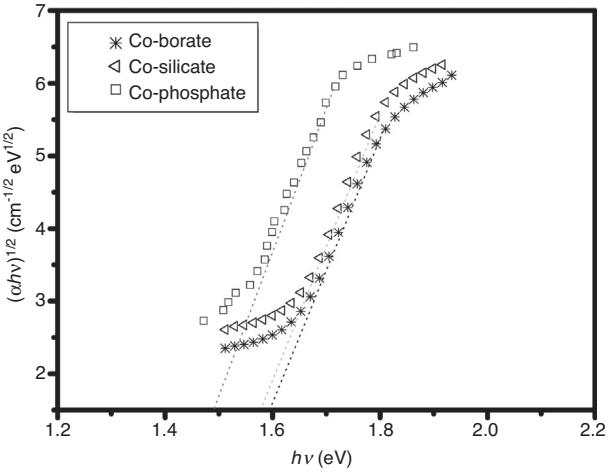

Fig. 10 – Optical band gap of CoO-doped glasses.

3.2.4. *Photoluminescence spectra of CuO doped glasses*

The emission spectra of 0.5% CuO-doped glasses, excited at 220 nm (in Fig. 8), show two strong broad emission bands extending from 425 to 600 nm in the visible light range; the first emission peak is centered at 464 nm and the other is centered at 556 nm. According to the octahedral crystal field, the Cu^{2+} ($3d^9$) loses its degeneracy and splits into ^2E_g and $^2T_{2g}$ with ^2E_g being the lower level. The luminescence spectra of CuO-doped glasses exhibit emission peaks at 420, 520 and 630 nm, which are assigned to $3d^94s \rightarrow 3d^{10}$ triplet transitions in Cu^{2+} ions [29–33].

4. Optical band gap (E_{opt}), Urbach energy (ΔE) and refractive index

Figs. 9–12 show the plots for indirect band gap of the prepared glasses. Energy gap and Urbach energy values are listed in Table 1. The values of optical mobility gap (E_{opt}) of iron, cobalt, nickel and copper ions doped glasses in the present work were found to be changeable within the range 2.444–1.490 eV. Table 1 reveals characteristic values of optical band gap, which are changeable between borate, silicate and phosphate containing

Table 1 – Calculated optical parameters of the prepared glasses.

Sample	Borate			Silicate			Phosphate		
	E_{opt} (eV)	ΔE (eV)	n	E_{opt} (eV)	ΔE (eV)	n	E_{opt} (eV)	ΔE (eV)	n
Fe	2.433	0.890	2.569	2.390	0.790	2.584	2.242	0.711	2.638
Co	1.594	0.660	2.937	1.579	0.590	2.945	1.490	0.250	2.998
Ni	2.335	0.749	2.603	2.035	0.386	2.721	1.801	0.257	2.827
Cu	2.444	0.610	2.565	2.314	0.125	2.611	2.200	0.368	2.654

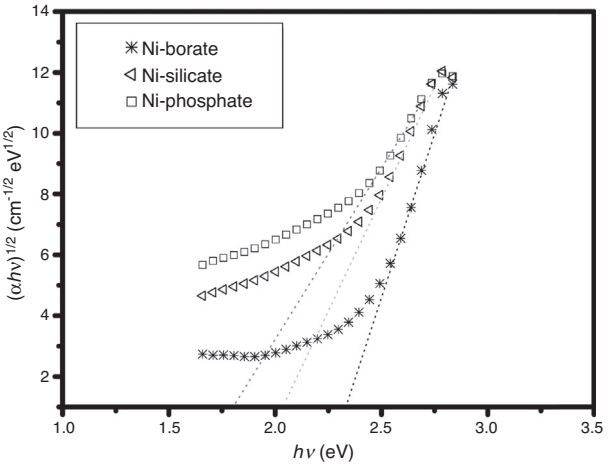

Fig. 11 – Optical band gap of NiO-doped glasses.

glasses. The calculated values of ΔE of the present glass systems are observed to be within the range of 0.125–0.89 eV for all the glasses. Mott and Davis [8] reported that, for amorphous materials to be semiconductor, ΔE values should lie between 0.045 and 0.67 eV. The recorded values of ΔE for both of the CoO and CuO-doped glasses, and NiO-doped silicate and phosphate reveal Urbach's energy values that are close to those of the semiconductors. Fe_2O_3-doped glasses and NiO-doped borate glass have not matched Mott and Davis [8] postulation. The variation of E_{opt} and ΔE could be attributed to the network structural differences brought about by the existence of

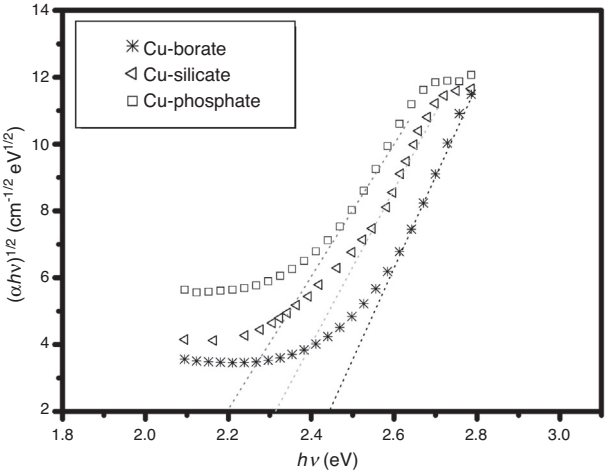

Fig. 12 – Optical band gap of CuO-doped glasses.

transition metal ions in different oxidation or coordination states [34].

The values of the refractive index thus obtained for all the glass samples are given in Table 1. The average value of refractive index, n, shows noticeable dependence on glass composition. The observed results indicate a slight successive increase in the refractive index from the borate to silicate to phosphate matrices. Generally, the increase of refractive index can be attributed to large atomic weight and coordinate number of Bi_2O_3 and the high polarizability of the Bi^{3+} ions in the glass system.

5. Contribution of the effect of transition metal ions and Bi_2O_3 on the photoluminescence and semiconducting behavior

It can be pointed out that bismuth doped borate, phosphate and silicate exhibit fluorescence emission centered at about 400 nm, which is attributed to the $^3P_1 \rightarrow {}^1S_0$ transition of Bi^{3+} ions [35–37]. The transition metal ions show enhanced photoluminescence of the studied heavy metal oxide glasses. This enhanced photoluminescence observed is due to energy transfer mechanism for both of the transition metal ion and Bi^{3+} from the ionic species of bismuth. It is also evident that the presence of high percent of PbO (60 mol%) and Bi_2O_3 (20 mol%) suppresses the effects of the 3d transition metal ions in their normal environments and, hence, they did not sharply or distinctly impart their known characteristics bands as they normally exhibit in alkali borate, alkali silicate, lead borate and lead silicate glasses [24–26,38].

The variation of E_{opt} and ΔE could be attributed to the network structural differences brought about by the existence of transition metal ions in different oxidation or coordination states. The transition metal ions enhance the non-bridging oxygens (NBOs) concentration and the states originating from NBOs are more easily excited than that of bridging oxygen atoms. Therefore, the increase in concentration of the NBO ions results in the shifting of valence band to higher energies and reduces the band gap energy [39]. From the comparison between all glass network formers, it is evident that the addition of Bi_2O_3 enhances the formation of octahedral groups, resulting in a highly cross-linked network, and thus causes the variations in the optical mobility gap between borate, silicate and phosphate glasses [2,18].

6. Conclusions

In the present study, transition metal ions of Fe_2O_3, CoO, NiO or CuO doped heavy metal oxide glasses having chemical

composition of $60PbO{\cdot}20Bi_2O_3{\cdot}20M_xO_y$ (where $M_xO_y = B_2O_3$ or SiO_2 or P_2O_5) were prepared by conventional melt annealing method. Photoluminescence and semiconducting properties have been measured and employed to evaluate the prepared glassy samples. The transition metal doped samples show strong UV-near visible bands that are related to the presence of Pb^{2+} and Bi^{3+} beside extra characteristic bands due to the respective transition metal ions. The observed emission spectra, recorded at 220 nm excitation, show two strong broad emission bands at about 462 and 550 nm for all glasses except CoO-doped glasses. The transition metal ions show enhanced photoluminescence of the studied heavy metal oxide glasses. Semiconducting behavior was found to be related to the type of transition metal ion and the glass network former existed in the glasses. The variation of E_{opt} and ΔE could be attributed to the network structural differences brought about by the existence of transition metal ions in different oxidation or coordination states. The increase of the refractive index can be attributed to large atomic weight and coordinate number of Bi_2O_3 and the high polarizability of the Bi^{3+} ions in the glass system.

Conflicts of interest

The authors declare no conflicts of interest.

REFERENCES

[1] Sahar MR, Budi AS. Optical band gap and IR spectra of glasses in the system $[Nd_2O_3]_{(x)}$–$[CuO]_{(35-x)}$–$[P_2O_5]_{(65)}$. Solid State Sci Technol 2006;14:115–20.

[2] ElBatal FH, Marzouk MA, Abdel Ghany AM. Gamma rays interaction with bismuth borate glasses doped by transition metal ions. J Mater Sci 2011;46:5140–52.

[3] Marzouk MA, Ouis MA, Hamdy YM. Spectroscopic studies and luminescence spectra of dy_2O_3 doped lead phosphate glasses. Silicon 2012;4:221–7.

[4] Chi GW, Zhou DC, Song ZG, Qiu JB. Effect of optical basicity on broadband infrared fluorescence in bismuth-doped alkali metal germanate glasses. Opt Mater 2009;31:945–8.

[5] Meng X, Qiu J, Peng M, Chen D, Zhao Q, Jiang X, et al. Near infrared broadband emission of bismuth-doped aluminophosphate glass. Opt Exp 2005;13:1628–34.

[6] Pan A, Ghosh A. A new family of lead–bismuthate glass with a large transmitting window. J Non-Cryst Solid 2000;271:157–61.

[7] Chimalawong P, Kaewkhao J, Limsuwan P. Optical investigation and electronic polarizability of Nd^{3+} doped soda-lime-silicate glasses. Energy Res J 2010;1(2):176–81.

[8] Mott N, Davis E. Electronic process in non-crystalline materials. 2nd ed. Oxford: Clarendon Press; 1979. p. 289.

[9] Sze SM. Semiconductor devices physics and technology. 3rd ed. Canada: John Wiley & Sons, Inc.; 2007.

[10] Bamford CR. Colour generation and control in glass. Glass science & technology, vol. 2. Amsterdam, The Netherlands: Elsevier; 1977.

[11] Urbach F. The long-wavelength edge of photographic sensitivity and of the electronic absorption of solids. Phys Rev 1953;92:1324.

[12] Dimitrov V, Sakka S. Electronic oxide polarizability and optical basicity of simple oxides I. J Appl Phys 1996;79(3):1736–40.

[13] Marzouk MA, Abo-Naf SM, Zayed HA, Hassan NS. Integration between optical and structural behavior of heavy metal oxide glasses doped with multiple glass formers. Silicon 2015, http://dx.doi.org/10.1007/s12633-015-9342-3.

[14] ElBatal FH. Gamma ray interaction with copper-doped sodium phosphate glasses. J Mater Sci 2008;43:1070–9.

[15] ElBatal HA, Abdelghany AM, ElBatal FH, ElBadry KM, Moustafa FA. UV–visible and infrared absorption spectra of gamma irradiated CuO-doped lithium phosphate, lead phosphate and zinc phosphate glasses: a comparative study. Physica B 2011;406:3694–703.

[16] Moustafa FA, Fayad AM, Ezz ElDin FM, El-Kashif I. Effect of gamma radiation on ultraviolet, visible and infrared studies of NiO, Cr_2O_3 and Fe_2O_3-doped alkali borate glasses. J Non-Cryst Solids 2013;376:18–25.

[17] ElBatal FH, Azooz MA, ElKheshen AA. UV–visible and infrared spectra of gamma-irradiated transition metals-doped lead borate glasses. Trans Indian Ceram Soc 2009;68(2):81–90.

[18] Marzouk MA. Optical characterization of some rare earth ions doped bismuth borate glasses and effect of gamma irradiation. J Mol Struct 2012;1019:80–90.

[19] Sundari GR, Sathish DV, Rao TR, Krishna CR, Reddy CV, Ravikumar RVSSN. Characterization of Fe^{3+} doped mixed alkali zinc borate glasses – physical and spectroscopic investigations. J Non-Cryst Solids 2013;365:6–12.

[20] Elbatal FH, Marzouk MA, Hamdy YM, ElBatal HA. Optical and FT infrared absorption spectra of 3d transition metal ions doped in NaF–CaF_2–B_2O_3 glass and effects of gamma irradiation. J Solid State Phys 2014;2014:1–8.

[21] Lakshminarayana G, Buddhudu S. Spectral analysis of Mn^{2+}, Co^{2+} and Ni^{2+}: B_2O_3–ZnO–PbO glasses. Spectrochim Acta A 2006;63:295–304.

[22] Buñuel MA, García J, Proietti MG, Solera JA, Cases R. Local structure of Ni^{2+} ions in fluorochloro- and fluorobromo-zirconate glasses. J Chem Phys 1999;110:3566–75.

[23] Bates T. Ligand field theory and absorption spectra of transition metal ions in glasses. In: Mackenzie JD, editor. Modern aspects of the vitreous state, vol. 2. London, UK: Butterworths; 1962. p. 195–254.

[24] Manjari VP, Krishna CR, Reddy CV, Begum SM, Reddy YP, Ravikumar RVSSN. Synthesis and characterization of undoped and Fe(III) ions doped $NaCaAlPO_4F_3$ phosphor. J Lumin 2014;145:324–9.

[25] Thulasiramudu A, Buddhudu S. Optical characterization of Mn^{2+}, Ni^{2+} and Co^{2+} ions doped zinc lead borate glasses. J Quant Spectrosc Radiat Transf 2006;102:212–27.

[26] Duan XL, Yuan DR, Cheng XF, Wang ZM, Sun ZH, Luan CN, et al. Absorption and photoluminescence characteristics of Co^{2+}P:$MgAl_2O_4$ nanocrystals embedded in sol–gel derived SiO_2-based glass. Opt Mater 2004;25:65–9.

[27] Naresh P, Raju GN, Rao CS, Prasad SVGVA, Kumar VR, Veeraiah N. Influence of ligand coordination of cobalt ions on structural properties of ZnO–ZnF_2–B_2O_3 glass system by means of spectroscopic studies. Physica B 2012;407:712–8.

[28] Mishra DK, Qi X. Energy levels and photoluminescence properties of nickel-doped bismuth ferrite. J Alloys Compds 2010;504:27–31.

[29] Rajyasree C, Teja PMV, Murthy KVR, Rao DK. Optical and other spectroscopic studies of lead, zinc bismuth borate glasses doped with CuO. Physica B 2011;406:4366–72.

[30] Chanshetti UB, Sudarsan V, Jogad MS, Chondhekar TK. Effect of CuO addition on the optical and electrical properties of sodium zinc borophosphate glasses. Physica B 2011;406:2904–7.

[31] Ignatovych M, Holovey V, Watterich A, Vidoczyd T, Baranyaid P, Kelemene A, et al. Luminescence characteristics of Cu- and Eu-doped $Li_2B_4O_7$. Radiat Measur 2004;38:567–70.

[32] Thulasiramudu A, Buddhudu S. Optical characterization of Cu^{2+} ion-doped zinc lead borate glasses. J Quant Spectrosc Radiat Transf 2006;97:181–94.
[33] Srinivasulu K, Omkaram I, Obeid H, Kumar AS, Rao JL. SpectralstudiesonCu^{2+} ions in sodium–lead borophosphate glasses. Physica B 2012;407:4741–5474.
[34] Ikhmayies SJ, Ahmad-Bitar RN. A study of the optical bandgap energy and Urbach tail of spray-deposited CdS:In thin films. J Mater Res Technol 2013;2(3):221–7.
[35] Singh SP, Karmakar B. Bismuth oxide and bismuth oxide doped glasses for optical and photonic applications. In: Bismuth: characteristics, production and applications. Materials science and technologies. New York: Nova, Hauppauge; 2012 [chapter 9].
[36] Xu W, Peng M, Ma Z, Dong G, Qiu J. A new study on bismuth doped oxide glasses. Opt Expr 2012;20(14):15692–702.
[37] Tabaza WAI, Swart HC, Kroon RE. Luminescence of Ce doped $MgAl_2O_4$ prepared by the combustion method. Physica B 2014;439:109–14.
[38] Ravikumar RVSSN, Chandrasekhar AV, Ramamoorthy L, Reddy BJ, Reddy YP, Yamauchi J, et al. Spectroscopic studies of transition metal doped sodium phosphate glasses. J Alloys Compds 2004;364:176–9.
[39] Marzouk MA, Ibrahim S, Hamdy YM. Luminescence efficiency growth in wide band gap semiconducting Bi_2O_3 doped $Cd_{0.4}Pb_{0.1}B_{0.5}$ glasses and effect of γ-irradiation. J Mol Struct 2014;1076:576–82.